

Magnetic correlations on the full chains of ortho-II $\text{YBa}_2\text{Cu}_3\text{O}_{6.5}$

W. Chen¹ and P. J. Hirschfeld²

¹*School of Physics, University of New South Wales, Sydney 2052, Australia*

²*Department of Physics, University of Florida, Gainesville, Florida 32611, USA*

(Received 26 November 2008; published 23 February 2009)

We propose that the NMR line shape on the chain Cu in the stoichiometric high- T_c superconductor ortho-II $\text{YBa}_2\text{Cu}_3\text{O}_{6.5}$ is determined by the magnetization induced on Cu near O vacancies due to strong magnetic correlations in the chains. An unrestricted Hartree-Fock calculation of a coupled chain-plane Hubbard model with nearest-neighbor d -wave pairing interaction shows that the broadening of NMR lines is consistent with disorder-induced magnetization at low temperatures. In addition, we give a possible explanation of the anomalous bimodal line shape observed at high temperatures in terms of nonuniform Cu valence in the chains. The proximity between chains and CuO plane induces anisotropic magnetization on the planar Cu and broadens the plane NMR lines in accordance with that of the chain lines, in agreement with experiment. We discuss implications of the model for other experiments on underdoped $\text{YBa}_2\text{Cu}_3\text{O}_{7-\delta}$.

DOI: [10.1103/PhysRevB.79.064522](https://doi.org/10.1103/PhysRevB.79.064522)

PACS number(s): 74.25.Bt, 74.25.Jb, 74.40.+k

I. INTRODUCTION

In materials with strong electronic correlations such as the cuprates, the response of the system to disorder can be quite different from weakly interacting metals. One well-known anomalous effect observed in disordered cuprates is the extended staggered magnetic droplets carrying a net moment which form around nonmagnetic impurities introduced on the CuO_2 plane. This picture was proposed on the basis of extensive NMR studies and can be understood within various theories of a potential scatterer in a correlated host metal.¹ The local susceptibility of these magnetic droplets manifests a Curie-Weiss behavior with a Weiss temperature which drops rapidly as the materials are underdoped.² While this picture was established for Zn, Li, and strong scatterers in the CuO_2 plane created by electron irradiation, the magnetic response to the weaker potentials created by out-of-plane dopants is also expected to be enhanced and has been claimed to be responsible for glassy behavior observed at low T and doping in intrinsically disordered systems such as $\text{La}_{1-x}\text{Sr}_x\text{CuO}_4$ and $\text{Bi}_2\text{Sr}_2\text{CaCu}_2\text{O}_8$.³ In such materials, it is generally believed that quasiparticles moving in the CuO_2 plane are subjected to weak extended potentials caused by the dopants, giving rise to small momentum-transfer scattering in the electronic transport.⁴⁻⁶

In the $\text{YBa}_2\text{Cu}_3\text{O}_{7-\delta}$ (YBCO) family, where most of the impurity-induced magnetization effects were studied, the system is doped in a different manner, which depends on the distribution of O atoms in the chain layers. Careful annealing under uniaxial pressure has been shown to give high-quality single crystals where the chain O is ordered with long correlation lengths.⁷ The so-called ortho-I, ortho-II, etc. YBCO crystals formed by these methods are the only known doped ordered stoichiometric high- T_c materials, which are ideal for studying the underlying intrinsic physics of the cuprates without complications from dopant disorder. It is then interesting to explore the effects of the few isolated defects which remain in these crystals, expected to be O vacancies in otherwise full CuO chains.⁸

The one-dimensional (1D) nature of the chains themselves induces, in the filled chain compound, a - b anisotropy which has been observed in dc^{9,10} and optical conductivity¹¹

and penetration depth measurements^{12,13} and is expected to affect the vortex core structure.¹⁴ Several authors^{15,16} have proposed that the anisotropy in penetration depth can be explained assuming a metallic chain that couples to the plane via interlayer hopping.¹⁷⁻²¹ The superconductivity observed in the chains is assumed to be due to the proximity coupling to the plane, where pairing occurs.²² While initially quantitative details of penetration depth disagreed with the proximity models, Atkinson²³ has argued that accounting for disorder can remove these discrepancies.

The presence of disorder has been shown to modify the local electronic structure of the chain layer. Scanning tunneling spectroscopy (STS) measurements on the chain layer of optimally doped YBCO show a clear conductance modulation,²⁴⁻²⁶ whose wavelength displays a strong energy dependence.²⁷ Such a dispersion in a quantity directly related to the local density of states (LDOS) suggests a Friedel-type oscillation description of this phenomenon, in contrast to an explanation in terms of a charge-density wave (CDW), which usually has a fixed wave vector. In addition, resonance peaks that appear in pairs are found at small frequencies, reminiscent of resonant magnetic impurity states in an unconventional superconductor. Morr and Balatsky²⁸ argued that such features could be caused by magnetic impurities in the chain layer, without discussing the origin of such defects.

In this paper we study the YBCO compound with a particular out-of-plane oxygen distribution, namely, the ortho-II structure of YBCO6.5 where every other chain is filled and show that the existence of magnetic correlations and their interplay with defects on the chain can explain a series of NMR experiments by Yamani *et al.*^{29,30} We show in Sec. II that the magnetization resulting from the Friedel oscillations of an uncorrelated system near the chain ends gives NMR linewidths much smaller than what has been reported. The linewidth in the uncorrelated case also remains temperature independent, contradicting the experimentally observed broadening with decreasing temperature. Including magnetic correlations in the chain layer within weak-coupling mean-field theory, we show that both the significantly larger linewidth and temperature dependence can be accounted for. This demonstrates the importance of magnetic correlations in the chains of YBCO systems, which is frequently neglected.

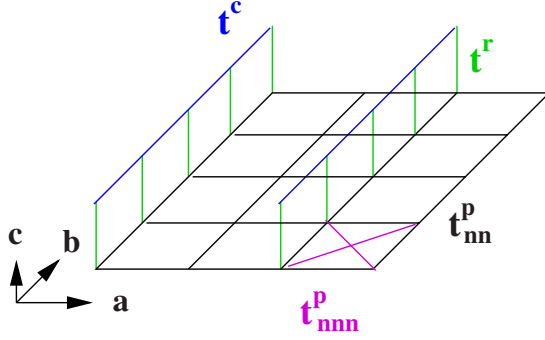


FIG. 1. (Color online) Schematic of chain-plane proximity model for ortho-II YBCO.

One of the unusual features of the line shape observed on the chain Cu's is a low-frequency satellite peak. We show here in Sec. III that satellite features do not arise naturally due to O chain vacancies, but it must be related to a set of sites in the material which have zero-spin shift. One possibility we discuss in some detail is that some of the chain Cu's are in the Cu^{3+} configuration.

In Sec. IV, we consider the coupling of the chain to the CuO_2 plane and show that the major effect of the chain-plane coupling is to induce an anisotropic magnetization pattern on the plane, where the chains imprint their 1D correlation length onto the plane. The broadening of plane NMR lines in accordance with that of chain NMR lines is reproduced in the proposed model, consistent with what is observed in the correlation between chain and plane linewidth in experiment.

II. MODEL HAMILTONIAN AND NMR SPECTRUM

The proper choice of a model for the ortho-II system relies on its unique lattice structure. Due to missing oxygen atoms on the empty chain, the Cu(1E) (chain Cu in "empty" chain) sites are highly localized and do not directly couple to the full chain; we therefore assume that they do not affect the magnetic properties on the full chain and drop these degrees of freedom. The resulting minimum effective model contains a single square lattice of Cu(2E) (planar Cu above empty chain site) and Cu(2F) (planar Cu above full chain site) where superconductivity occurs and couples to evenly spaced one-dimensional chains via interlayer hopping, as shown in Fig. 1. The full Hamiltonian consists of

$$H = H_p + H_c + H_{\text{inter}} + H_{\text{imp}}, \quad (1)$$

where H_p describes the planar hopping, pairing, and magnetic correlations

$$H_p = \sum_{ij\sigma} -t_{ij}^p \hat{c}_{i\sigma}^\dagger \hat{c}_{j\sigma} + \sum_{i\sigma} (\epsilon_\sigma^p - \mu^p) \hat{n}_{i\sigma}^p \quad (2)$$

$$+ \sum_i U^p \hat{n}_{i\uparrow}^p \hat{n}_{i\downarrow}^p - \sum_{\langle ij \rangle} V \hat{n}_{i\uparrow}^p \hat{n}_{j\downarrow}^p, \quad (3)$$

and on the chain layer

$$H_c = \sum_{x\sigma} -t^c (\hat{d}_{x\sigma}^\dagger \hat{d}_{x+\delta\sigma} + \text{H.c.}) \quad (4)$$

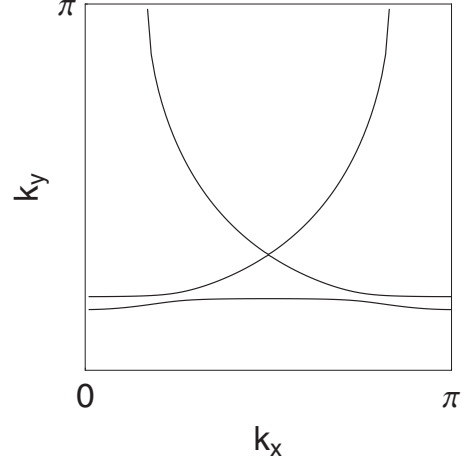


FIG. 2. Fermi surface produced by the model described in Fig. 1 with parameters $(t_{nn}^p=1, t_{nnn}^p=-0.4, t^c=2, t^r=0.1, \mu^p=-1.1, \mu^c=-3.25)$, and we take $t_{nn}^p=150$ meV.

$$+ \sum_{x\sigma} (\epsilon_\sigma^c - \mu^c) \hat{n}_{x\sigma}^c + \sum_x U^c \hat{n}_{x\uparrow}^c \hat{n}_{x\downarrow}^c, \quad (5)$$

with the coupling between them

$$H_{\text{inter}} = \sum_{\langle ix \rangle \sigma} -t^r (\hat{c}_{i\sigma}^\dagger \hat{d}_{x\sigma} + \text{H.c.}) \quad (6)$$

We denote by $\hat{c}_{i\sigma}$ ($\hat{d}_{x\sigma}$) the plane (chain) operator located at site i (x) and by t_{ij}^p (t^c) the planar (chain) hopping, with on site Coulomb repulsion U^p (U^c) on the plane (chain). The chain hopping is only between nearest neighbors, while planar hopping t_{ij}^p contains both nearest- t_{nn}^p and next-nearest-neighbor sites t_{nnn}^p , which is necessary to produce the Fermi surface of the YBCO system. The short-range attractive interaction V accounts for the d -wave pairing in the plane, and the effect of magnetic field is included in the Zeeman term $\epsilon_\sigma^{p/c} = g\mu_B B/2$. The proper choice of all parameters except the U 's relies on three criteria: (1) the Fermi surface of ortho-II calculated from density-functional theory (DFT)^{31,32} is reproduced in this simple three-site model, (2) the homogeneous magnetization on the full chains is consistent with the value indicated by the main line of Cu(1F) NMR spectrum, and (3) a critical temperature of $T_c=60$ K is obtained. Regarding the first point, Fig. 2 shows the Fermi surface produced by the present model in the normal state with $V=0$. Although one does not expect the splitting of the plane band, since the chains are connected to a single plane in this minimum model, the topology and the folding of the Brillouin zone is well reproduced. Notice that the chain band is almost parallel to the zone boundary with a very small intercept $k_y \sim \pi/4$, indicating the small filling of the conduction electrons on the chain, which is a natural result of fitting the complex Fermi surface by this simple tight-binding model. We therefore choose the chemical potential such that the average chain filling is 0.25, and the average plane filling is 0.9. Since the main line of the NMR spectrum is given by the sites far from the defects, if one assumes a dilute impurity concentration, we found that $t^c=2$ gives a Knight shift and magnetization consistent with the value corresponding to the measured

Cu(1F) main line, which then fixes the absolute scale of the bandwidth for the chain. Finally, $T_c=60$ K in the presence of the chosen interlayer hopping fixes the pairing interaction at $V=0.5$, and the absolute scale of our energy unit t_{nn}^p is chosen such that the magnetic field scale and temperature dependence of the NMR lines are consistent with experiments, which gives $t_{nn}^p=150$ meV.

A Hartree-Fock-Gorkov mean-field factorization is then applied to the above Hamiltonian, with order parameters defined as

$$\begin{aligned} n_i^p &= \langle \hat{n}_{i\uparrow}^p + \hat{n}_{i\downarrow}^p \rangle, \\ m_i^p &= \langle \hat{n}_{i\uparrow}^p - \hat{n}_{i\downarrow}^p \rangle, \\ \Delta_{\delta i} &= V \langle c_{i\uparrow} c_{i+\delta\downarrow} \rangle, \\ n_x^c &= \langle \hat{n}_{x\uparrow}^c + \hat{n}_{x\downarrow}^c \rangle, \\ m_x^c &= \langle \hat{n}_{x\uparrow}^c - \hat{n}_{x\downarrow}^c \rangle. \end{aligned} \quad (7)$$

A Bogoliubov transformation is applied for both chain and plane operators

$$\begin{aligned} c_{i\uparrow} &= \sum_n u_{n,i\uparrow}^p \gamma_{n\uparrow} + v_{n,i\uparrow}^{p*} \gamma_{n\uparrow}^\dagger, \\ c_{i\downarrow} &= \sum_n u_{n,i\downarrow}^p \gamma_{n\downarrow} + v_{n,i\downarrow}^{p*} \gamma_{n\downarrow}^\dagger, \\ d_{x\uparrow} &= \sum_n u_{n,x\uparrow}^c \gamma_{n\uparrow} + v_{n,x\uparrow}^{c*} \gamma_{n\uparrow}^\dagger, \\ d_{x\downarrow} &= \sum_n u_{n,x\downarrow}^c \gamma_{n\downarrow} + v_{n,x\downarrow}^{c*} \gamma_{n\downarrow}^\dagger, \end{aligned} \quad (8)$$

and the order parameters are determined by the following self-consistent equations:

$$\begin{aligned} \langle c_{i\uparrow}^\dagger c_{i\uparrow} \rangle &= \sum_{n>0} |u_{n,i\uparrow}^p|^2 f(E_{n\uparrow}) + |v_{n,i\uparrow}^p|^2 [1 - f(E_{n\downarrow})], \\ \langle c_{i\downarrow}^\dagger c_{i\downarrow} \rangle &= \sum_{n>0} |u_{n,i\downarrow}^p|^2 f(E_{n\downarrow}) + |v_{n,i\downarrow}^p|^2 [1 - f(E_{n\uparrow})], \\ \langle d_{x\uparrow}^\dagger d_{x\uparrow} \rangle &= \sum_{n>0} |u_{n,x\uparrow}^c|^2 f(E_{n\uparrow}) + |v_{n,x\uparrow}^c|^2 [1 - f(E_{n\downarrow})], \\ \langle d_{x\downarrow}^\dagger d_{x\downarrow} \rangle &= \sum_{n>0} |u_{n,x\downarrow}^c|^2 f(E_{n\downarrow}) + |v_{n,x\downarrow}^c|^2 [1 - f(E_{n\uparrow})], \\ \langle c_{i\uparrow} c_{i+\delta\downarrow} \rangle &= \sum_{n>0} u_{n,i\uparrow}^p v_{n,i+\delta\downarrow}^{p*} [1 - f(E_{n\uparrow})] + v_{n,i\uparrow}^{p*} u_{n,i+\delta\downarrow}^p f(E_{n\downarrow}), \\ \langle d_{x\uparrow} d_{x+\delta\downarrow} \rangle &= \sum_{n>0} u_{n,x\uparrow}^c v_{n,x+\delta\downarrow}^{c*} [1 - f(E_{n\uparrow})] + v_{n,x\uparrow}^{c*} u_{n,x+\delta\downarrow}^c f(E_{n\downarrow}), \end{aligned} \quad (9)$$

where $n > 0$ indicates only eigenstates with positive eigenenergies are included in the summation. Note that by estimating

the concentration of terminal Cu, the average chain length that produces reported NMR spectrum was reported to be around $120b$, where b is the chain lattice constant by Yamani *et al.*^{29,30} We therefore simulate such a system by a rectangular plane with size 12×121 , where each odd chain allows for hopping along its length of 121 sites directed along the x direction.

The resonance frequency ν_i at site i is calculated by converting magnetization to Knight shift K_{spin} ,

$$\begin{aligned} S_x &= \frac{1}{2} \langle n_{x\uparrow} - n_{x\downarrow} \rangle = \frac{\chi_x B}{g \mu_B}, \\ \chi_x &= \frac{K_{\text{spin}} \mu_B}{A_{\text{hf}}}, \end{aligned} \quad (10)$$

which yields, when combined with the orbital shift K_{orb} , the local resonance frequency

$$\nu_x = \frac{\gamma}{2\pi} B \left[1 + K_{\text{orb}} + S_x \left(\frac{g A_{\text{hf}}}{B} \right) \right]. \quad (11)$$

For Cu(1F) NMR lines, we use $A_{\text{hf}}=80$ kOe, $g=2$, $K_{\text{orb}}=1.2\%$, and $\gamma/2\pi=11.285$ MHz/T. The histogram of collecting ν_i on all Cu(1F) sites is then artificially broadened by a Lorentzian to give a continuous spectrum

$$I(\nu) = \frac{1}{R} \sum_{\nu_x} N(\nu_x) \frac{1}{\pi} \frac{\eta}{(\nu - \nu_x)^2 + \eta^2}, \quad (12)$$

where $N(\nu_i)$ is number of sites that have frequency ν_i , with $\eta=0.04$, and R is the proper numerical factor that normalizes the area under the $I(\nu)$ curve.

We now examine different impurity models that are relevant to the NMR experiments. The most straightforward proposal for H_{imp} comes from the observation that the chain hopping is a result of orbital overlap between Cu(1F) and its two adjacent oxygen atoms, such that abrupt termination of the full chain due to missing oxygen atoms should dramatically reduce the hopping at the chain ends. A single isolated reduction in t^c is modeled by an additional term in the Hamiltonian

$$H_{\text{imp}}^{(1)} = \sum_{\sigma} -\delta t^c (d_{l\sigma}^\dagger d_{l+\delta\sigma} + \text{H.c.}) \quad (13)$$

with a further assumption of complete elimination $\delta t^c = -t^c$ and one impurity per chain. The Cu(1F) line caused by a single hopping reduction in the chain layer is shown in Fig. 3, where we highlight the effect of magnetic correlation U^c with the model containing only $H_{\text{chain}} + H_{\text{imp}}^{(1)}$, to isolate the chain from proximity to the plane in the first analysis.

The parameter range explored for U^c is such that it is close but smaller than the critical value beyond which the system flows into long-range magnetic order in the presence of impurities and the induced moment remains in the paramagnetic region. Figure 3 shows that the broadening of the Cu(1F) line coincides with the enhancement of real-space magnetization as U^c is increased, while the linewidth for the uncorrelated case $U^c=0$ is significantly smaller. The periodicity of magnetic oscillation, as well as the density modula-

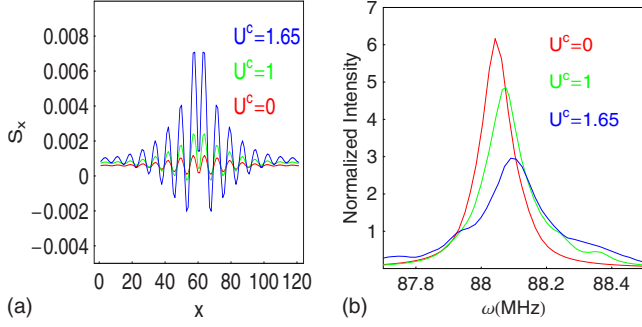


FIG. 3. (Color online) Magnetization (left) and NMR spectrum (right) produced by reduction in a single hopping in an isolated 1D chain (located at the middle of the chain as shown), equivalent to Hamiltonian $H_{\text{chain}} + H_{\text{imp}}^{(1)}$, in an external field of 7.7 T at 50 K. The enhancement of magnetization is consistent with the broadening of NMR linewidth as U^c is increased.

tion for electrons of both spin species, is on the order of ten lattice constants from the defect, consistent with the small Fermi momentum of the chain band $k_y \sim \pi/4$ resulting from fitting the Fermi surface with the three-site model. Moreover, the temperature dependence of the linewidth shown in Fig. 4 indicates that only the correlated case can properly account for the experimentally observed broadening as temperature is lowered, while the width in the uncorrelated case remains constant. The linewidth plus its temperature dependence therefore proves the existence of magnetic correlations on the full chains of the ortho-II YBCO6.5. Our best fit to the linewidth gives $U^c = 1.65$ and will be the value used for the rest of the paper unless otherwise specified. We make detailed comparison with experiment in Sec. IV.

III. SATELLITE FEATURE IN CHAIN Cu NMR LINE

Although the Cu(1F) linewidth and temperature dependence is well described by impurity-induced magnetization due to U^c , one important feature regarding the Cu(1F) line shape seems to be outside of this scheme. At temperature higher than 70 K or so, a satellite peak with significant weight gradually develops at frequency slightly lower than the main line.³⁰ Our calculations for a single defect or chain

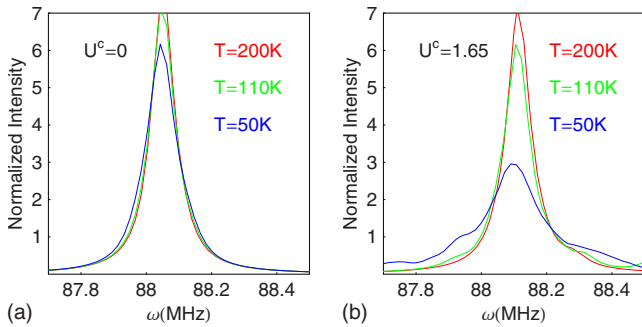


FIG. 4. (Color online) Temperature dependence of an NMR lines for an isolated chain with sparse bond impurities, $H_{\text{chain}} + H_{\text{imp}}^{(1)}$, for an uncorrelated chain (left) and the correlated case (right).

end indicate that magnetization decays smoothly away from the chain ends, however, leading to no particular satellite explanation for the satellite peak observed. Two aspects of this high-temperature satellite appear to us to be important: (1) the weight of the peak is about 10% of the whole spectrum and (2) the position of the peak remains roughly the same at all temperatures. Aspect (1) then implies that roughly 10% of the sample has the same magnetization value, which results in this satellite peak. Aspect (2) suggests that this magnetization remains constant at high temperature. Since increasing temperature should continuously reduce any finite magnetization developed due to the correlation effect, it is reasonable to assume that this observed constant magnetization is zero. In fact, the frequency of this satellite peak corresponds very closely to an NMR shift ν with zero Knight shift $K_{\text{spin}} = 0$. We therefore propose that the high-temperature satellite peak is due to a section of adjacent chain Cu which has their conduction electrons missing, i.e., Cu^+ ions. The valence changes may be correlated with the chain ends due to the change in local chemical environment which prohibits electrons from populating these sites, but need not be. Indeed the valence of the Cu(1) ions has been controversial, and our analysis suggests that the valence may be distributed quite inhomogeneously. Eliminating these adjacent Cu(1F) Cu in the one-band model gives the following perturbation:

$$H_{\text{imp}}^{(2)} = \sum_{1 \leq l \leq L, \sigma} -\delta t^c (d_{l\sigma}^\dagger d_{l+\delta} + \text{H.c.}) + \sum_{1 \leq l \leq L, i, \sigma} -\delta t^r (\hat{c}_{i\sigma}^\dagger \hat{d}_{l\sigma} + \text{H.c.}) + \sum_{1 \leq l \leq L, \sigma} U_{\text{imp}} \hat{n}_{l\sigma}^c, \quad (14)$$

where $\delta t^c = -t^c$ eliminates the hopping between these chain sites and $\delta t^r = -t^r$ eliminates the interlayer hopping that connects the plane sites with these chain sites. A strong impurity potential $U_{\text{imp}} = 100$ is introduced to artificially project out electrons on these sites. Notice that the summation over impurity position in Eq. (14) is arbitrarily restricted between a section of adjacent sites $1 \leq l \leq L$ with $L = 15$.

The effect of removing these Cu spins is first examined in a single isolated chain, where the elimination of δt^r in Eq. (14) is omitted since all couplings to the plane are ignored in this approximation. In comparison with randomly distributed missing oxygen atoms $H_{\text{chain}} + H_{\text{imp}}^{(1)}$, Cu(1F) lines given by considering $H_{\text{chain}} + H_{\text{imp}}^{(2)}$ show a clear asymmetric line shape with significantly more weight at lower frequency, as shown in Fig. 5. The zero magnetization peak appears at all temperatures and is specially noticeable at high temperature as the main line narrows. Broadening of the main line smears out the satellite peak, which may explain its apparent disappearance at low temperature in the work of Yamani *et al.*³⁰ A typical real-space magnetization pattern of the eliminated Cu(1F) model is shown in Fig. 6, where one can clearly identify each sector of the magnetization with the corresponding features in the NMR spectrum.

IV. EFFECT OF CHAIN-PLANE COUPLING

The conclusion from examining the single isolated chain does not alter as the chains are coupled to the plane; in other

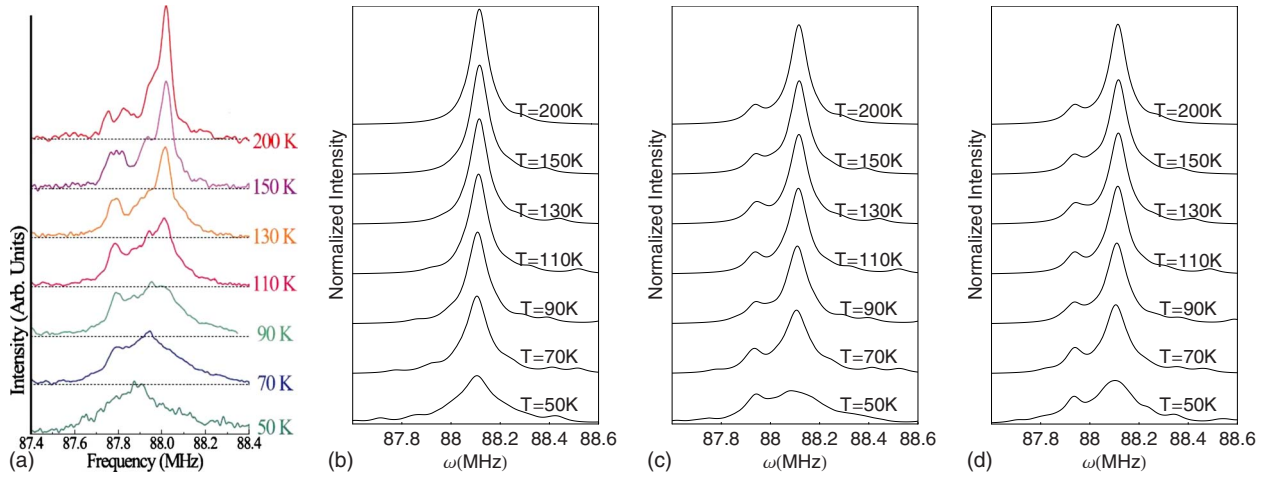


FIG. 5. (Color online) Comparison of experimental $^{63}\text{Cu}(1\text{F})$ NMR line of ortho-II YBCO6.5 at external field of 7.7 T along the a direction (upper left), with three models studied: isolated 1D chain with random impurities $H_{\text{chain}} + H_{\text{imp}}^{(1)}$ (upper right), isolated 1D chain with a section of consecutive Cu erased $H_{\text{chain}} + H_{\text{imp}}^{(2)}$ (lower left), and chain-plane coupled system with a section of chain Cu erased $H_{\text{plane}} + H_{\text{chain}} + H_{\text{inter}} + H_{\text{imp}}^{(2)}$ (lower right).

words, we still see (1) broadening of spectrum at low temperature, (2) asymmetric spectral weight, and (3) the high-temperature satellite peak, as shown in Fig. 5. The interlayer coupling influences the pairing and magnetic state of the plane, as we show below, but as far as the chain magnetization is concerned, the interlayer coupling does not qualitatively affect its magnitude or spatial distribution.

Our basic finding here is that the chain magnetization, which has a strongly 1D character, imprints itself on the magnetic response of the plane to which it is coupled, even though the coupling itself is only via interplanar hopping (there are no explicit chain-plane exchange interactions included in the Hamiltonian). Disorder in the plane will of course produce a response with local two-dimensional (four-fold) symmetry, as in, e.g., the occasional Cu vacancy which will produce a unitary scatterer. We neglect these effects in the current model and focus only on the chain disorder which is expected to dominate in the ultraclean ortho-II crystals.

To demonstrate this pronounced planar 1D anisotropy, as well as to compare with the planar unitary scatterers, we employed again the reduction in a single hopping on the

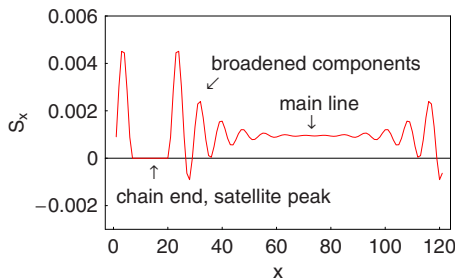


FIG. 6. (Color online) Real-space magnetization on one of the chains in the Cu(1F) model $H_{\text{plane}} + H_{\text{chain}} + H_{\text{inter}} + H_{\text{imp}}^{(2)}$ at temperature of 70 K. The spinless sites, here assumed to be near the chain end, give zero magnetization and correspond to the satellite peak on the NMR spectrum. The small magnetization region away from the chain end corresponds to the main line, while the large oscillation sector close to the spinless sites broadens the main line.

chain $H_{\text{imp}}^{(1)}$ as discussed in Sec. II but this time consider the full chain-plane system $H_{\text{plane}} + H_{\text{chain}} + H_{\text{inter}} + H_{\text{imp}}^{(1)}$. Figure 7 shows the resulting magnetization pattern induced on both chain layer and the plane, where one again sees the long-wavelength oscillation associated with the small Fermi momentum of the chain band, similar to the result of Fig. 3. In addition, the proximity between the two layers inherits this small chain Fermi momentum to the plane and results in a small planar induced magnetization that has wavelength similar to that of the chain. The planar magnetization is obviously directed along the chain direction, which confirms our suspicion that out-of-plane oxygen disorder in YBCO can induce anisotropic density and magnetic modulations on the plane. On the other hand, numerics show that if one places a unitary scatterer on the plane, then the anisotropy of its induced magnetization is much smaller even when interlayer coupling is present. Such a hierarchy unambiguously proves that, when systems with different dimensions are coupled, the response of lower dimension can drive that of the higher dimension, consistent with our expectation that correlation effect becomes more significant as dimensionality is lowered.

Finally, we address the issue of correlation between broadening of Cu(1F) and Cu(2E/F) lines. Experimentally the identification of each line on the complete NMR spectrum is made via comparison with YBCO6 and YBCO7 spectra, and the Knight shift can be extracted by subtracting the orbital contribution K_{orb} associated with each copper species.²⁹ The reverse process provides the recipe of recovering the NMR spectrum in the present model, with each line calculated by collection of magnetization and Eq. (11). The value of K_{orb} at external field $B \parallel \mathbf{b}$ is taken from Takigawa *et al.*³³ In Fig. 8, we show that the broadening of extracted Cu(2F) and Cu(2E) lines as temperature is lowered follows that of Cu(1F), with the slope of Cu(2E) smaller than that of Cu(2F). Increasing the interlayer hopping increases the Cu(1F) and Cu(1E) linewidths, indicating that the magnetization on the plane comes from its proximity to the chains. Within the range of interlayer hopping that retains the Fermi-

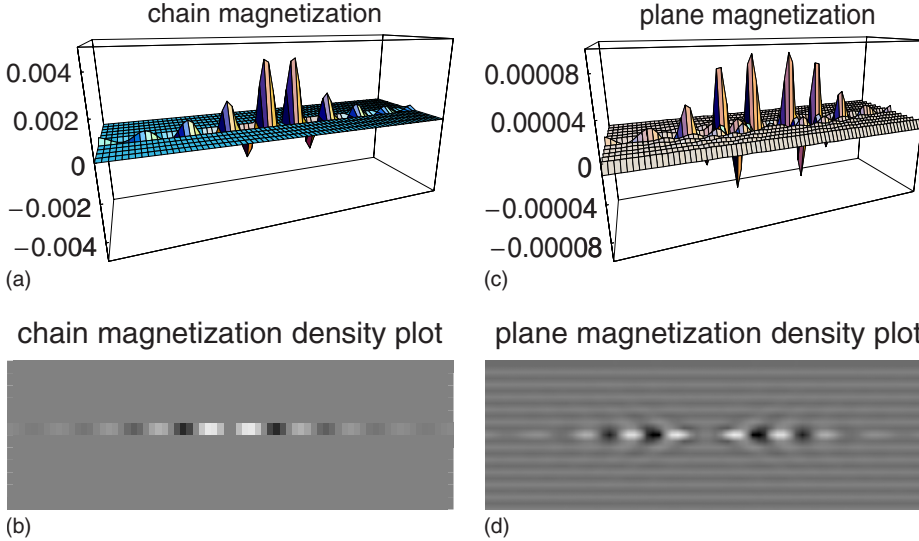


FIG. 7. (Color online) Magnetization induced (a) on the chain layer and (b) on the plane by a hopping reduction defect $H_{\text{imp}}^{(1)}$ located on a single chain, together with their corresponding false color plots (c) and (d) which manifest the similarity between their periodicity. The size of the plane is 72×24 at a temperature of 70 K.

surface topology, the linewidth correlation between the planar Cu and the chain Cu is roughly linear, similar to the conclusion found experimentally.³⁰

V. CONCLUSIONS

In summary, we have shown that the broadening of Cu(1F) NMR lines of ortho-II YBCO in the superconducting state at low temperatures cannot be explained unless one assumes the existence of intermediate strength magnetic correlations on the chains. We presented a model with correlations described by Hubbard interactions U on both the plane and chains, together with a d -wave pairing interaction, both of which were treated in an unrestricted mean-field approximation. In the presence of an impurity, here assumed to be an oxygen vacancy in the nearly full chain, we find that a staggered incommensurate magnetization oscillation grows as temperature is lowered (see Ref. 1); many such defects give rise to a broadening of NMR lines which grows as tempera-

ture is decreased, in quantitative agreement with recent experiments by Yamani *et al.*^{29,30} The Friedel-type spin-density wave induced by an uncorrelated metallic host is, by contrast, too small and temperature independent and therefore cannot account for the broadening of NMR lines.

Such a simple model based on impurity-induced magnetism in a correlated host does not, however, explain the high-temperature satellite feature observed in the NMR spectrum on ortho-II samples in Refs. 29 and 30. We therefore further proposed an *ad hoc* modification which may account for this feature, by assuming a set of few percent Cu(1F) 3+ ions in the chains. The essential point is that these exceptional Cu's should produce zero polarization; this then accounts quite well for the weight and temperature independences of the observed satellite peaks. This may point to a hitherto unanticipated clustering of valence inhomogeneities in the nearly filled chains.³⁴

In addition, our model assumes pairing interactions in the plane alone, and superconductivity is induced in the chains only by “proximity coupling,” i.e., a chain-plane electron hopping. This coupling is then found to cause an imprint of the defect-induced magnetic chain correlations on the plane itself, consisting of an incommensurate spin-density wave of quasi-1D character. This signal is 1 order of magnitude smaller than the chain polarization for realistic parameters but should still be observable.³⁵ Indeed, within our model the broadening of planar NMR lines is proportional to that of the chain NMR line, consistent with the observation by Yamani *et al.*^{29,30} These defect-induced 1D correlations should enhance the effect of the chain bands on the magnetic response of the YBCO system at low energies, particularly for low dopings near the ortho-II and -III oxygen concentrations where an integer number of chains are filled.³⁶ Further research into various aspects of this response is in progress.

ACKNOWLEDGMENTS

We gratefully acknowledge useful discussions with Z. Yamani, W. A. Atkinson, D. A. Bonn, J. Bobroff, J. P. Carbotte, P. Dai, M. Gabay, W.N. Hardy, Y. Sidis, and O.P. Sushkov.

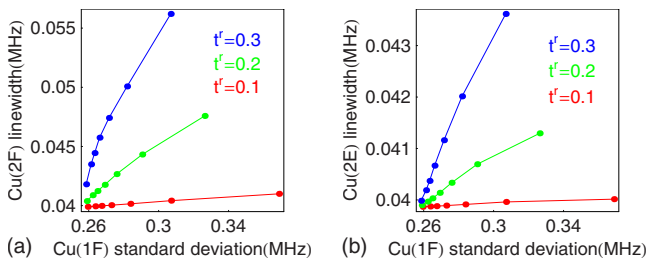


FIG. 8. (Color online) The standard deviation of Cu(1F) line versus the Lorentzian linewidth of the (a) Cu(2F) and (b) Cu(2E) lines, extracted from the chain-plane model $H_{\text{plane}} + H_{\text{chain}} + H_{\text{inter}} + H_{\text{imp}}^{(2)}$. Note that due to the high-temperature satellite peak and the complex line shape of Cu(1F), as shown in Fig. 5, we use the standard deviation of the Cu(1F) line to represent its linewidth. Data are taken at system size 101×10 with eliminated sites $L=11$ in impurity model (14), and the temperature of each point corresponds to the same scale in Fig. 5.

- ¹H. Alloul, J. Bobroff, M. Gabay, and P. J. Hirschfeld, *Rev. Mod. Phys.* **81**, 45 (2009).
- ²J. Bobroff, H. Alloul, W. A. MacFarlane, P. Mendels, N. Blanchard, G. Collin, and J.-F. Marucco, *Phys. Rev. Lett.* **86**, 4116 (2001).
- ³B. M. Andersen, P. J. Hirschfeld, A. P. Kampf, and M. Schmid, *Phys. Rev. Lett.* **99**, 147002 (2007).
- ⁴H.-Y. Kee, *Phys. Rev. B* **64**, 012506 (2001).
- ⁵E. Abrahams and C. M. Varma, *Proc. Natl. Acad. Sci. U.S.A.* **97**, 5714 (2000).
- ⁶L. Zhu, P. J. Hirschfeld, and D. J. Scalapino, *Phys. Rev. B* **70**, 214503 (2004).
- ⁷R. Liang, D. A. Bonn, and W. N. Hardy, *Physica C* **336**, 57 (2000).
- ⁸J. S. Bobowski, P. J. Turner, R. Harris, R. Liang, D. A. Bonn, and W. N. Hardy, *Physica C* **460-462**, 914 (2007).
- ⁹T. A. Friedmann, M. W. Rabin, J. Giapintzakis, J. P. Rice, and D. M. Ginsberg, *Phys. Rev. B* **42**, 6217 (1990).
- ¹⁰R. Gagnon, C. Lupien, and L. Taillefer, *Phys. Rev. B* **50**, 3458 (1994).
- ¹¹D. N. Basov, R. Liang, D. A. Bonn, W. N. Hardy, B. Dabrowski, M. Quijada, D. B. Tanner, J. P. Rice, D. M. Ginsberg, and T. Timusk, *Phys. Rev. Lett.* **74**, 598 (1995).
- ¹²Kuan Zhang, D. A. Bonn, S. Kamal, Ruixing Liang, D. J. Baar, W. N. Hardy, D. Basov, and T. Timusk, *Phys. Rev. Lett.* **73**, 2484 (1994).
- ¹³J. L. Tallon, C. Bernhard, U. Binniger, A. Hofer, G. V. M. Williams, E. J. Ansaldo, J. I. Budnick, and Ch. Niedermayer, *Phys. Rev. Lett.* **74**, 1008 (1995).
- ¹⁴W. A. Atkinson and J. E. Sonier, *Phys. Rev. B* **77**, 024514 (2008).
- ¹⁵T. S. Nunner, B. M. Andersen, A. Melikyan, and P. J. Hirschfeld, *Phys. Rev. Lett.* **95**, 177003 (2005).
- ¹⁶T. S. Nunner and P. J. Hirschfeld, *Phys. Rev. B* **72**, 014514 (2005).
- ¹⁷W. A. Atkinson and J. P. Carbotte, *Phys. Rev. B* **52**, 10601 (1995).
- ¹⁸W. A. Atkinson and J. P. Carbotte, *Phys. Rev. B* **55**, 14592 (1997).
- ¹⁹C. O'Donovan and J. P. Carbotte, *Phys. Rev. B* **55**, 1200 (1997).
- ²⁰R. Combescot, *Phys. Rev. B* **57**, 8632 (1998).
- ²¹D. K. Morr and A. V. Balatsky, *Phys. Rev. Lett.* **87**, 247002 (2001).
- ²²T. Xiang and J. M. Wheatley, *Phys. Rev. Lett.* **76**, 134 (1996).
- ²³W. A. Atkinson, *Phys. Rev. B* **59**, 3377 (1999).
- ²⁴H. L. Edwards, J. T. Markert, and A. L. de Lozanne, *Phys. Rev. Lett.* **69**, 2967 (1992).
- ²⁵H. L. Edwards, A. L. Barr, J. T. Markert, and A. L. de Lozanne, *Phys. Rev. Lett.* **73**, 1154 (1994).
- ²⁶H. L. Edwards, D. J. Derro, A. L. Barr, J. T. Markert, and A. L. de Lozanne, *Phys. Rev. Lett.* **75**, 1387 (1995).
- ²⁷D. J. Derro, E. W. Hudson, K. M. Lang, S. H. Pan, J. C. Davis, J. T. Markert, and A. L. de Lozanne, *Phys. Rev. Lett.* **88**, 097002 (2002).
- ²⁸D. K. Morr and A. V. Balatsky, *Phys. Rev. Lett.* **90**, 067005 (2003).
- ²⁹Z. Yamani, W. A. MacFarlane, B. W. Statt, D. Bonn, R. Liang, and W. N. Hardy, *Physica C* **405**, 227 (2004).
- ³⁰Z. Yamani, B. W. Statt, W. A. MacFarlane, Ruixing Liang, D. A. Bonn, and W. N. Hardy, *Phys. Rev. B* **73**, 212506 (2006).
- ³¹A. Carrington and E. A. Yelland, *Phys. Rev. B* **76**, 140508(R) (2007).
- ³²E. Bascones, T. M. Rice, A. O. Shorikov, A. V. Lukoyanov, and V. I. Anisimov, *Phys. Rev. B* **71**, 012505 (2005).
- ³³M. Takigawa, P. C. Hammel, R. H. Heffner, and Z. Fisk, *Phys. Rev. B* **39**, 7371 (1989).
- ³⁴J. Bobroff, W. A. MacFarlane, H. Alloul, P. Mendels, N. Blanchard, G. Collin, and J.-F. Marucco, *Phys. Rev. Lett.* **83**, 4381 (1999).
- ³⁵S. Ouazi, J. Bobroff, H. Alloul, and W. A. MacFarlane, *Phys. Rev. B* **70**, 104515 (2004).
- ³⁶S. Ouazi, J. Bobroff, H. Alloul, M. Le Tacon, N. Blanchard, G. Collin, M. H. Julien, M. Horvatic, and C. Berthier, *Phys. Rev. Lett.* **96**, 127005 (2006).